Mott transition in bosonic systems: Insights from the variational approach

Manuela Capello,[1] Federico Becca,[2,3] Michele Fabrizio,[2,3,4] and Sandro Sorella[2,3]

[1] Laboratoire de Physique Théorique, Université Paul Sabatier, CNRS, 31400 Toulouse, France
[2] International School for Advanced Studies (SISSA), I-34014 Trieste, Italy
[3] CNR-INFM-Democritos National Simulation Centre, Trieste, Italy.
[4] International Centre for Theoretical Physics (ICTP), P.O. Box 586, I-34014 Trieste, Italy

We study the Mott transition occurring for bosonic Hubbard models in one, two, and three spatial dimensions, by means of a variational wave function benchmarked by Green's function Monte Carlo calculations. We show that a very accurate variational wave function, constructed by applying a long-range Jastrow factor to the non-interacting boson ground state, can describe the superfluid-insulator transition in any dimensionality. Moreover, by mapping the quantum averages over such a wave function into the the partition function of a classical model, important insights into the insulating phase are uncovered. Finally, the evidence in favor of anomalous scenarios for the Mott transition in two dimensions are reported whenever additional long-range repulsive interactions are added to the Hamiltonian.

I. INTRODUCTION

The recent advances achieved on cold atoms trapped in optical lattices have generated an increasing interest in the condensed matter community, since they allow experimental realizations of simple lattice models.[1,2] A great advantage of these systems is the possibility to have a direct control of the parameters, such as the width of the bands and the strength of the interactions, that can be manipulated by varying the depth of the optical potential.[3] Therefore, cold atoms on optical lattices give the unique opportunity to make a close contact with theoretical models and to examine the origin of the fundamental physical phenomena that occur in crystalline materials. In particular, one of the most spectacular example is given by the superfluid-insulator transition in a system of interacting bosons: The so-called Mott transition.[2]

In this paper, we consider the superfluid-insulator transition in a bosonic system with different kinds of interactions. The simplest model that contains the basic ingredients of strong correlations is the Hubbard model

$$\mathcal{H} = -\frac{t}{2} \sum_{\langle i,j \rangle} b_i^\dagger b_j + h.c. + \frac{U}{2} \sum_i n_i(n_i - 1), \quad (1)$$

where $\langle \dots \rangle$ indicates nearest-neighbor sites, $b_i^\dagger$ (b_i) creates (destroys) a boson on the site i, and $n_i = b_i^\dagger b_i$ is the local density operator. Here, we consider N particles on a one-dimensional (1D) chain, a two-dimensional (2D) square lattice, and a three-dimensional (3D) cubic lattice with L sites and periodic-boundary conditions. At zero temperature and integer densities $\rho = N/L$ there is a superfluid-insulator transition when the ratio between the kinetic energy and the on-site interaction is varied. Otherwise, for non-integer fillings, the ground state is always superfluid. In a seminal paper,[4] by using a field-theoretical approach, Fisher and coworkers proposed that the transition of the d-dimensional clean system belongs to the XY universality class in $d + 1$. This

scenario has been confirmed mostly in one and two dimensions by using different numerical techniques, such as quantum Monte Carlo and density-matrix renormalization group.[5,6,7,8,9] In particular, it has been verified that in one dimension at $\rho = 1$ there is a Kosterlitz-Thouless transition and the estimation of the critical value of the on-site interaction ranges between $U_c/t \sim 1.7$ and $U_c/t \sim 2.3$.[5,7] Instead, a second-order phase transition is claimed to occur for $U_c/t \sim 8.5$ in two dimensions,[9] and for $U_c/t \sim 14.7$ in three dimensions.[10]. Accurate estimations for the critical values can be also obtained from a strong-coupling expansion.[11,12]

Besides the numerically exact techniques, important insights into the various phases can be obtained by considering simplified variational wave functions. The simplest example is given by the celebrated Gutzwiller state, where the on-site correlation term allows for the suppression of the energetically expensive charge fluctuations. Contrary to the fermionic case, when considering bosons, it is possible to deal with this wave function without any further approximation.[13,14] Then, the Mott transition is obtained with a reasonable estimate of the corresponding critical value U_c/t, namely $U_c/t = d(\sqrt{n_c} + \sqrt{n_c + 1})^2$ for integer fillings $\rho = n_c$. The main drawback of this approach is that, similarly to what happens with fermions, the transition is reached with a vanishing kinetic energy and the insulating state completely lacks charge fluctuations, namely all particles are localized, n_c in each lattice site. Of course, this leads to a wrong description of the insulator, whenever the local interaction is finite.

Following the ideas of previous works on fermionic systems,[15,16,17] in a recent paper[18] we have shown that, in order to correct this outcome and obtain a more accurate description of the ground state, it is necessary to include a long-range Jastrow factor, whose singular behavior at small momenta was shown to be able to turn a non-interacting bosonic state into an insulator that still contains density fluctuations. In this paper, we present

a more detailed study of the properties of that Jastrow wave function, as well as of its accuracy in comparison with Green's function Monte Carlo (GFMC) calculations, which, because of the absence of the sign problem, provide numerically exact results.[19,20]

The same Jastrow wave function turns out to be also very effective to describe Hamiltonians that contain long-range interactions. This case has not been considered much in the literature, and we will show that different scenarios for the superfluid-insulator transition could occur. As a matter of fact, long-range interactions have been studied mostly in the continuum, where a transition between a charged bosonic fluid and a Wigner crystal has been found by varying the density.[21,22,23] In particular, in the presence of a logarithmic repulsion, the 2D Bose liquid was found to have no condensate fraction, due to the predominance of long-wavelength plasmon excitations.[21] In the last part of this paper, we generalize the Hubbard model of Eq. (1) to

$$\mathcal{H}_{LR} = -\frac{t}{2} \sum_{\langle i,j \rangle} b_i^\dagger b_j + h.c. + \frac{V}{2} \sum_{i,j} \Omega(R_i, R_j) n_i n_j, \quad (2)$$

where $\Omega(R_i, R_j)$ is a long-range potential that only depends upon the relative distance $|R_i - R_j|$ between two particles and V represents its strength. In particular, we will consider two possibilities for the long-range potential. The first one is obtained by taking the Coulomb interaction between (charged) bosons moving in a 2D lattice embedded in a three-dimensional environment, which leads to the following potential in reciprocal space

$$\Omega(q_x, q_y) = \frac{\pi}{\sqrt{(\cos q_x + \cos q_y - 3)^2 - 1}}, \quad (3)$$

with a small-q behavior $\Omega(q) \sim 1/|q|$. The second case consists in directly considering the solution of the Poisson equation in 2D:

$$\Omega(q_x, q_y) = \frac{1}{2 - (\cos q_x + \cos q_y)}, \quad (4)$$

which for small momenta behaves like $\Omega(q) \sim 1/q^2$, leading to a logarithmic interaction in real space, i.e., $\Omega(r) \sim -\log(r)$. In both cases, a uniform background is considered in order to cancel the divergent $q = 0$ component of the potential.

The paper is organized as follow: In section II, we describe the variational wave function, in sections III, IV and V, we show the results for the 1D, 2D and 3D short-range models. Then, in section VI, we consider the 2D case with long-range interactions and finally, in section VII, we draw our conclusions.

II. THE VARIATIONAL WAVE FUNCTION

A. The Jastrow wave function

The variational wave function is defined by applying a density Jastrow factor to a state with all the bosons condensed into the $q = 0$ state

$$|\Psi_J\rangle = \exp\left\{-\frac{1}{2} \sum_{ij} v_{i,j}(n_i - 1)(n_j - 1)\right\} |\Phi_0\rangle, \quad (5)$$

where $|\Phi_0\rangle = (\sum_i b_i^\dagger)^N |0\rangle$ is the non-interacting boson ground state with N particles, $(n_i - 1)$ is the variation of the on-site density with respect to the average value $\rho = 1$, and $v_{i,j}$ are translationally invariant parameters that can be optimized to minimize the variational energy.[24] In order to get some physical insight from the variational state, it is more instructive to consider the Fourier transform of the Jastrow parameters v_q. Indeed, there is a tight connection between the small-q behavior of v_q and the nature of the ground state. In particular, as we are going to discuss, $v_q \sim 1/|q|$ implies the existence of sound modes in any dimensions, as expected in a superfluid. On the contrary, to recover an insulating behavior a much more singular v_q for $q \to 0$ is required.[18] The physical reason is that, in order to describe a realistic Mott insulating wave function that does include charge fluctuations, it is necessary to spatially correlate the latters. This is accomplished by a sufficiently singular v_q that favors configurations where opposite-sign fluctuations, $(n_i - 1)(n_j - 1) < 0$, are close to each other, while equal-sign ones, $(n_i - 1)(n_j - 1) > 0$, are far apart.

It should be mentioned that previous studies of fermionic systems[25] and more recent ones on the bosonic Hubbard model,[26] stressed the importance of a many-body term containing holon-doublon interactions for nearest-neighbor sites:

$$|\Psi_{g,MB}\rangle = \exp\left(-g \sum_i n_i^2 + g_{MB} \sum_i \xi_i\right) |\Phi_0\rangle, \quad (6)$$

where g and g_{MB} are variational parameters and the many-body operator is defined by

$$\xi_i = h_i \prod_\delta (1 - d_{i+\delta}) + d_i \prod_\delta (1 - h_{i+\delta}), \quad (7)$$

where $h_i = 1$ ($d_i = 1$) if the site i is empty (doubly occupied) and 0 otherwise, $\delta = \pm x, \pm y$; therefore, ξ_i counts the number of isolated holons (empty sites) and doublons (doubly occupied sites). Even though this operator has been originally introduced for fermionic systems, where the maximum occupancy at each site is given by two electrons, it is useful also for bosons, since in the limit of large U/t the number of sites with an occupation larger than two is negligible. However, within this framework, the evidence for a true Mott transition is rather controversial, and it is not clear if an insulating phase can be stabilized in the thermodynamic limit.[26]

Combining together the variational Eqs. (5) and (6),

we obtain the variational ansatz

$$|\Psi_{J,MB}\rangle = \exp\left\{-\frac{1}{2}\sum_{i,j} v_{i,j}(n_i - 1)(n_j - 1)\right.$$
$$\left. + g_{MB}\sum_i \xi_i\right\}|\Phi_0\rangle, \quad (8)$$

containing both the long-range Jastrow factor and a short-range many-body term. As it will be shown in the next sections, the presence of the latter term is important in 2D and 3D, mainly to increase the accuracy in the strong-coupling regime. Instead, in 1D, the many-body term does not improve the accuracy of the long-range Jastrow state and there is no appreciable difference between the wave function (5) and (8). In any case, we emphasize that, according to our calculations, the short-range term alone cannot lead to an insulating behavior, and the main ingredient to drive a superfluid-insulator transition is the long-range Jastrow factor, parametrized by v_q.

B. Mapping onto a classical model

The variational calculation with the wave function (8) can be shown to correspond to a classical problem at finite temperature. This correspondence provides many insights into the properties of $|\Psi_{J,MB}\rangle$. To prove the mapping, let us denote a bosonic configuration by the positions $\{x\}$ of the particles and a generic quantum state by $|\Psi\rangle$. For all the operators θ diagonal in space coordinates, the quantum average

$$\langle\theta\rangle = \frac{\langle\Psi|\theta|\Psi\rangle}{\langle\Psi|\Psi\rangle} \quad (9)$$

can be written in terms of the *classical* distribution $|\Psi(x)|^2 = |\langle x|\Psi\rangle|^2 / \sum_{x'}|\langle x'|\Psi\rangle|^2$, as

$$\langle\theta\rangle = \sum_x \langle x|\theta|x\rangle |\Psi(x)|^2. \quad (10)$$

Since $|\Psi(x)|^2$ is a positive quantity, there is a precise correspondence between the wave function and an effective classical potential $V_{cl}(x)$:

$$|\Psi(x)|^2 = e^{-V_{cl}(x)}. \quad (11)$$

The explicit form of the potential $V_{cl}(x)$ depends upon the choice of the Jastrow factor, while $|\Phi_0\rangle$ does not contribute to it, since $\langle x|\Phi_0\rangle$ does not depend upon the configuration $|x\rangle$. In particular, whenever there is only the two-body potential (i.e., $g_{MB} = 0$) $V_{cl}(x)$ is Gaussian, i.e., $V_{cl}(x) = \sum_{q\neq 0} v_q n_q(x) n_{-q}(x)$, being $n_q(x)$ the Fourier transform of the local density of the configuration $|x\rangle$. In this case, the variational problem becomes equivalent to solve a classical model of oppositely charged particles (the holons and the doublons) mutually interacting

through a potential determined by v_q. In the presence of the short-range many-body term, $V_{cl}(x)$ is no longer Gaussian. However, when the density fluctuations are suppressed at large U/t, the quadratic term gives the most relevant contribution, hence the mapping onto a classical model of interacting oppositely charged particle still holds with $V_{cl}(x) \sim \sum_{q\neq 0} v_q^{eff} n_q(x) n_{-q}(x)$, v_q being replaced by a slightly different effective potential v_q^{eff}. In spite of the differences, it is plausible that the small-q behavior of v_q^{eff} must follow the same singular behavior of the Jastrow potential v_q.

Let us now discuss in more details the connection between the form of v_q and the low-energy excitation spectrum of the system. By means of the f-sum rule one can show that[18,27]

$$E_q = -2\frac{\langle k\rangle}{DN_q}\sum_{i=1}^{D}\sin^2\left(\frac{q_i}{2}\right) = \frac{\int d\omega\,\omega\,N(q,\omega)}{\int d\omega\,N(q,\omega)}, \quad (12)$$

where $N(q,\omega)$ is the dynamical structure factor, $N_q = \int d\omega\,N(q,\omega)$ the static one, and $\langle k\rangle$ the hopping energy per site. E_q can be interpreted as the average excitation energy of density fluctuations at momentum q. $E_q \to 0$ for $q \to 0$ is a sufficient but not necessary condition for the existence of gapless excitations. In particular, deep inside the superfluid phase, E_q must coincide with the energy dispersion of the Bogoliubov sound mode, which carries most of the spectral weight. Although we can not access directly dynamical properties by our variational wave function, still we can provide a variational estimate of E_q, in the same spirit of the Feynmann's construction in liquid Helium.[28] This amounts to use the variational values of $\langle k\rangle$ and of the static structure factor N_q, defined as

$$N_q = \frac{\langle\Psi|n_q n_{-q}|\Psi\rangle}{\langle\Psi|\Psi\rangle}, \quad (13)$$

with n_q the Fourier transform of the local density. Note that the uncorrelated

$$N_q^0 = \frac{\langle\Phi_0|n_{-q}n_q|\Phi_0\rangle}{\langle\Phi_0|\Phi_0\rangle} \quad (14)$$

is constant for any $q \neq 0$ at $\rho = 1$. Whenever a weak-coupling approach in the Jastrow potential v_q is possible, the following relation holds:[29]

$$N_q = \sum_x n_q(x)\,n_{-q}(x)\,e^{-V_{cl}(x)} \sim \frac{N_q^0}{1 + 2N_q^0 v_q} \sim \frac{1}{v_q}, \quad (15)$$

the last equality following from the singular behavior of v_q that is expected both in the superfluid and in the Mott insulating phases. Eq. (15) shows that $v_q \sim 1/|q|$ allows to recover the correct behavior of $N_q \sim |q|$ and $E_q \sim |q|$ in the superfluid regime, which is what we indeed find, see following sections. In the insulating phase, should Eq. (15) be valid, we would expect $v_q \sim \beta/q^2$

to get the expected behavior $N_q \sim q^2$ and E_q finite for small q. This would correspond through Eq. (11) to a classical Coulomb gas model (CGM) with effective temperature $T_{eff} = \pi/\beta$.[30] In 1D, for any finite temperature, the CGM is always in a confined phase where oppositely charged particles are tightly bound in pairs, and with exponential decaying correlation functions.[31] This suggests that the 1D CGM may indeed provide through the mapping (11) a good description of a 1D Mott insulating wave function.

In 2D the CGM undergoes a Berezinskii-Kosterlitz-Thouless phase transition at $T_c^{CGM} \sim 1/4$, between a confined phase (stable at low temperature) and a plasma phase (stable at high temperature). Similarly to the 1D case, one would argue that the confined phase should correspond to the 2D Mott insulator. However, the 2D confined phase of the CGM displays power-law decaying correlations[30] that would correspond to power-law decaying equal-time correlations of the quantum ground state. This is not compatible with a genuine Mott insulator, which already suggests that the insulating wave function must be characterized by a Jastrow potential v_q more singular than $1/q^2$ as $q \to 0$, as indeed we find. In turns, this implies that (15) must not be valid, since, in spite of $v_q \times q^2 \to \infty$ for $q \to 0$, we still expect $N_q \sim q^2$.

The breakdown of Eq. (15) becomes even more pronounced in 3D, where a potential $v_q \sim 1/q^2$ cannot describe at all an insulator since it is not sufficiently singular to empty the condensate fraction.[32] In fact, we find that the optimized variational wave function shows a more diverging $v_q \sim 1/|q|^3$ in the 3D insulator,[18] though $N_q \sim q^2$. The properties connected to the insulating phase can be again uncovered within a classical 3D gas with a $1/|q|^3$ potential, recently considered in Ref. 33. Indeed, analogously to what happens in 2D, also in 3D a system of charges interacting with a logarithmic potential in real space admits a high-temperature fluid regime separated by a low-temperature dielectric phase. Within this mapping, the 3D insulating state is found to correspond to the low-temperature phase of this classical model.

In the following, we will present our results obtained by considering the quantum variational wave function and we will use the classical mapping to gain insights into the ground-state properties. Moreover, in order to verify the accuracy of the variational calculations, we will perform the numerically exact GFMC that allows one to obtain ground-state properties.

III. THE 1D HUBBARD MODEL

Here, we consider a chain of L sites with periodic boundary conditions and $N = L$ bosons. First of all, in Fig. 1 we compare the variational accuracy of the wave functions (5), (6) and (8) for different values of U/t. Once a long-range Jastrow factor is considered, the many-body term of Eq. (7) is irrelevant and there is no appreciable
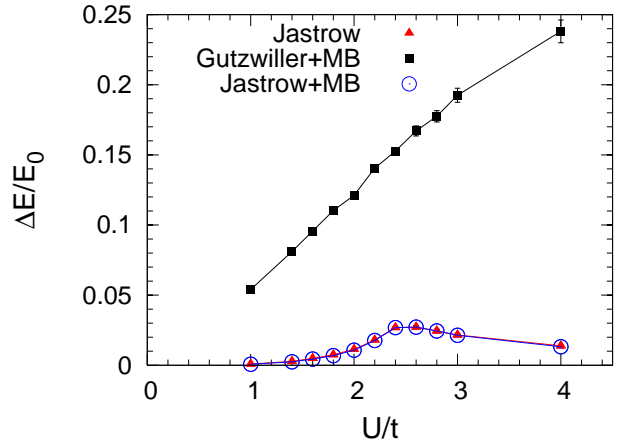

FIG. 1: Accuracy of different variational wave functions as a function of U/t for 60 sites and 60 bosons. $\Delta E = E_0 - E_{VMC}$, where E_{VMC} is the variational energy and E_0 is the ground-state one, obtained by GFMC. The state of Eq. (5) is denoted by "Jastrow", the one of Eq. (6) by "Gutzwiller+MB", and the one of Eq. (8) by "Jastrow+MB".
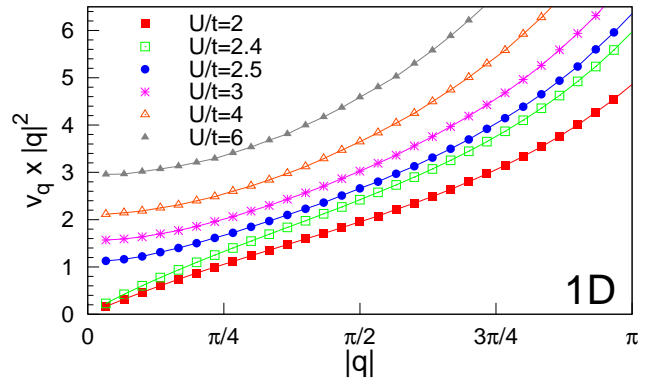

FIG. 2: Jastrow parameters v_q multiplied by q^2 as a function of $|q|$ for 60 sites and 60 bosons.

difference between the wave functions (5) and (8), for all the values of the on-site interaction. By contrast, the Gutzwiller state, also when supplied by the many-body term, is much less accurate by increasing U/t.

Therefore, in the following, we will consider the state with long-range Jastrow factor (5) alone, since the many-body term makes the algorithm much slower and does not improve the quality of the variational state. In Fig 2, we report the minimized Jastrow parameters v_q multiplied by q^2 for different U/t: There is a clear difference in the small-q behavior for $U/t \lesssim 2.4$, where $v_q \sim \alpha/|q|$ and for $U/t \gtrsim 2.5$, where $v_q \sim \beta/q^2$. At the variational level, the change of the singular behavior of the Jastrow parameters for $U/t \sim 2.45$ marks the superfluid-insulator transition. Indeed, as discussed in the previous paragraph, $v_q \sim \alpha/|q|$ implies a gapless system, whereas $v_q \sim \beta/q^2$ indicates a finite gap in the excitation spectrum. Let
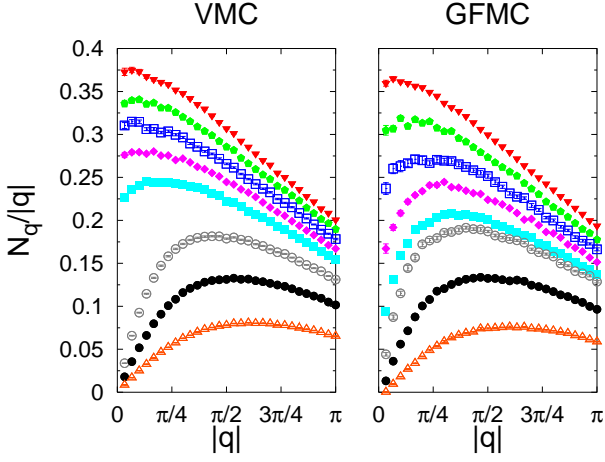
FIG. 3: Density structure factor N_q divided by $|q|$ calculated with variational Monte Carlo (left panel) and GFMC (right panel) for different U/t and $L = 60$. From top to bottom $U/t = 1.6$, 1.8, 2, 2.2, 2.4, 2.5, 3, and 4.

FIG. 4: Variational results for the momentum distribution $\mathbf{n}_k$ in 1D for $L = 60$ (squares), 100 (circles), and 150 (triangles) across the transition ($U/t = 2.4$ and 2.5). Inset: Size scaling of the condensate fraction $\mathbf{n}_0/L$ for $U/t = 2.4$ (upper curve) and $U/t = 2.5$ (lower curve).

us now concentrate on the insulating phase. Here, the Jastrow wave function (5) can be mapped onto the partition function of an effective classical CGM and β plays the role of the inverse classical temperature $\beta = \pi/T_{eff}$. In 1D the CGM is in the confined phase for any finite temperature, with exponential correlations.[31] This outcome is consistent with the fact of having, in the quantum model, a finite gap in the excitation spectrum. Remarkably close to the Mott transition in the insulating phase, the value of β obtained from the optimized Jastrow potential is very small and approaches to zero when $U \to U_c$ from above. Since the correlation length of the 1D CGM diverges for $\beta \to 0$, our numerical outcome gives a strong indication in favor of a continuous transition between the superfluid and the Mott insulating phase.

Let us now analyze the transition by considering the density structure factor N_q. In the small-q regime, we can generally write that

$$N_q = \gamma_1 |q| + \gamma_2 q^2 + O(q^3), \qquad (16)$$

where γ_1 and γ_2 depend upon the Jastrow parameters. In analogy with spin systems, we have that $\gamma_1 = v_c\chi$, with v_c and χ the sound velocity and the compressibility, respectively. The fact of having $\gamma_1 = 0$ in the insulating regime indicates that this state is incompressible (i.e., $\chi = 0$). From Fig. 3, we obtain that γ_1 has a very sharp crossover from a finite value to zero across the transition, suggestive of a true jump in the thermodynamic limit. This outcome is consistent with the fact that the compressibility also has a finite jump in the 1D quantum phase transition.[34] Moreover, just above U_c in the insulating regime, γ_2 is very large for both the variational and the GFMC calculations, indicating the peculiar character of the 1D transition. By using the small-q behavior of the density structure factor, the Mott transition can be located at $U_c/t \sim 2.45 \pm 0.05$ for the variational calculation, whereas the GFMC approach gives $U_c/t \sim 2.1 \pm 0.1$.
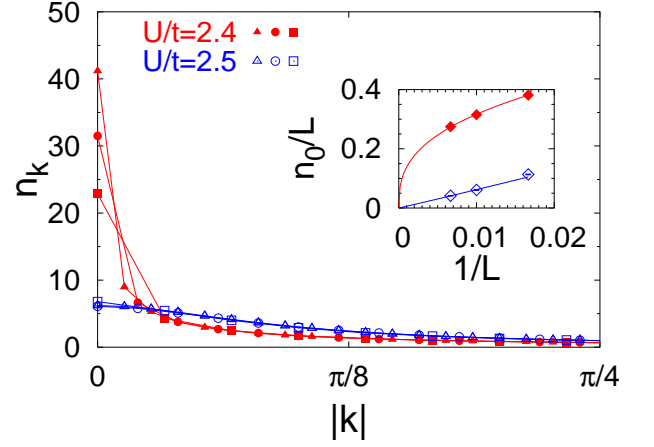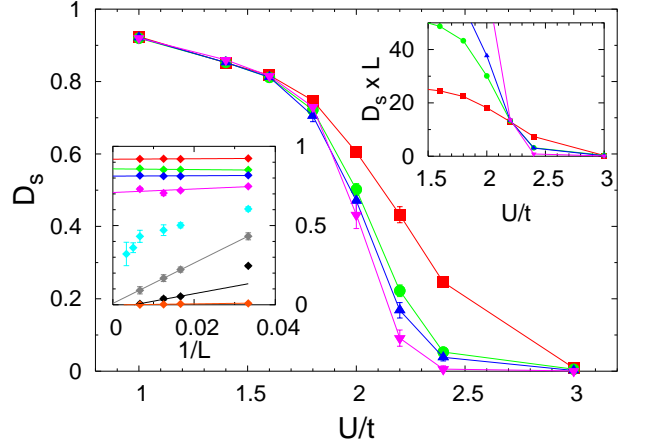

FIG. 5: Superfluid stiffness D_s calculated by GFMC as a function of U/t for different sizes in the 1D boson Hubbard model. Lower inset: Size scaling of D_s for different U/t (same values of the main panel, with U/t increasing from top to bottom). Upper inset: $D_s \times L$ as a function of U/t. The point where the different curves cross marks the transition point.

The superfluid-insulator transition can be also easily detected by considering the momentum distribution:

$$\mathbf{n}_k = \frac{\langle \Psi_J | b_k^\dagger b_k | \Psi_J \rangle}{\langle \Psi_J | \Psi_J \rangle}, \qquad (17)$$

where $b_k^\dagger$ is the creation operator of a boson of momentum k. This quantity has a radically different behavior below and above the transition: In the superfluid phase, it has a cusp at $k = 0$, although there is no condensate fraction, i.e., $\mathbf{n}_0/L \to 0$ for $L \to \infty$, while in the insulating phase it is a smooth function of the momentum k, see Fig. 4.

Finally, we want to conclude the 1D part by considering the superfluid stiffness D_s. In analogy to what has been done by Pollock and Ceperley at finite temperature,[35] this quantity can be also calculated directly at zero temperature by using the GFMC and the so-called winding numbers (see Appendix)

$$D_s = \lim_{\tau \to \infty} \frac{\langle \Psi_0 | |\vec{W}(\tau)|^2 | \Psi_0 \rangle}{D \, L \, \tau}, \qquad (18)$$

where $|\Psi_0\rangle$ is the ground-state wave function obtained by GFMC, D is the dimension of the system and $\vec{W}(\tau) = \sum_i [\vec{r}_i(\tau) - \vec{r}_i(0)]$, $\vec{r}_i(\tau)$ being the position of the i-th particle after evolving it for a diffusion time τ from the initial position $\vec{r}_i(0)$. The diffusion process must be done without considering periodic boundary conditions, namely by increasing or decreasing the values of the coordinates of a particle that crosses the boundaries of the cluster. In this way, non-zero winding numbers across the lattice can be detected. It should be stressed that, exactly at zero temperature, D_s can only give information about the presence of a gap in the excitation spectrum, and, therefore, it can discriminate between conducting and insulating phases. Our results show that D_s is finite and large in the weak-coupling regime, whereas it vanishes for $U/t \gtrsim 2.1$, see Fig. 5. Again, in analogy with spin systems and from general scaling arguments valid for 1D boson models, we expect a jump at the transition, that however is very hard to detect by considering finite clusters.[34] Nevertheless, an accurate value of the transition point is obtained from the size scaling of $D_s \times L$, see Fig. 5.

IV.   THE 2D HUBBARD MODEL

Let us now turn to the 2D Hubbard model and consider square clusters with $L = l \times l$ sites and $N = L$ bosons. The accuracy of the three wave functions (5), (6) and (8) are reported in Fig. 6. The situation is different from the previous 1D case: The Gutzwiller state with the many-body term, which in 1D is not accurate for large U/t, in 2D becomes competitive with the Jastrow wave function for $U/t \gtrsim 14$. Moreover, the presence of the many-body term strongly improves the accuracy of the Jastrow state as soon as $U/t \gtrsim 8$. Then, in the following, we will consider the state (8) for both the variational and the GFMC calculations.

In Fig. 7, we show the behavior of the optimized v_q as a function of the interaction strength. Similarly to what happens in the 1D system, we obtain that $v_q \sim \alpha/|q|$ for $U/t \lesssim 10.5$, while v_q is best fitted by $v_q \sim -\log(q)/q^2$ for $U/t \gtrsim 10.5$ (see Fig. 8), corresponding to the superfluid and the Mott insulating phase, respectively. As we anticipated in section II B, the Jastrow potential in the insulating phase is more singular than $1/q^2$, suggestive of a classical model with bound charges but presumably without the power-law correlations displayed by the CGM
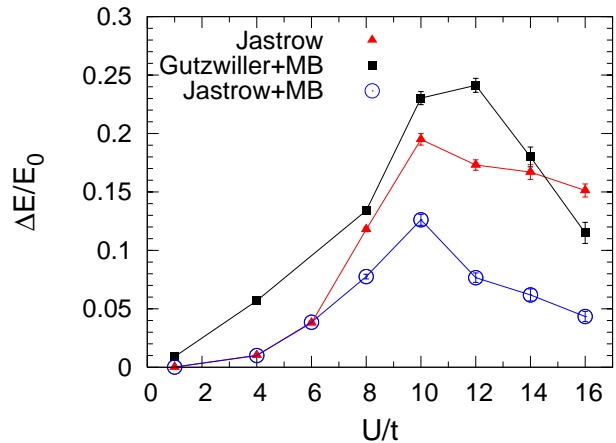

FIG. 6: Accuracy of different variational wave functions as function of U/t for the 10×10 cluster and 100 bosons. The symbols are the same as in Fig. 1.
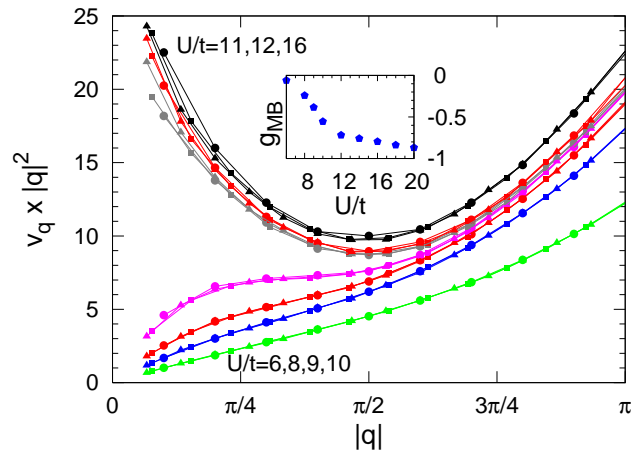

FIG. 7: Jastrow parameters v_q multiplied by q^2 as a function of $|q|$ [along the (1,0) direction] for 20×20 (circles), 26×26 (squares), and 30×30 (triangles) clusters. Inset: The many-body variational parameter g_{MB} as a function of U/t.

in the confined phase. In reality, on the sizes available to our numerical approach, we can not firmly establish whether a classical potential $-\log(q)/q^2$ has indeed exponential decaying correlation functions. Nevertheless, it is remarkable and very encouraging that the variational optimization leads to such a singular v_q.

The evidence that the change in behavior of v_q does correspond to the superfluid-insulator transition comes also by the small-q limit of the structure factor N_q. In Fig. 9, we show the results for the variational and the GFMC calculations as a function of U/t. In both cases, we find a different small-q behavior for large and small couplings. In the variational calculations, for $U/t \lesssim 10.3$ the structure factor behaves as $N_q \sim \gamma_1|q|$, while for $U/t \gtrsim 10.3$ we get $N_q \sim \gamma_2 q^2$. Therefore, at the variational level, the superfluid-insulator transition is located around $U_c/t \sim 10.3 \pm 0.1$; this value is slightly smaller
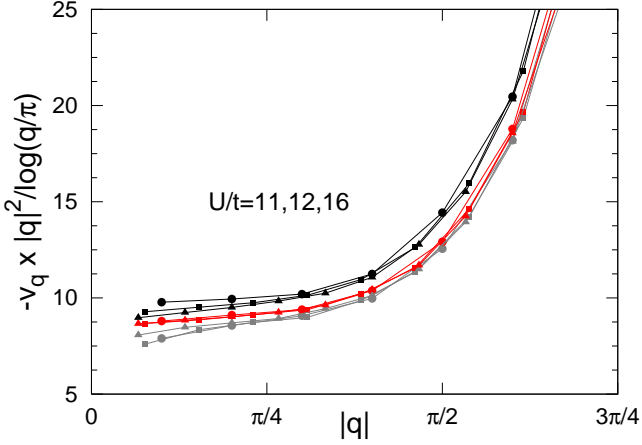
FIG. 8: Jastrow parameters v_q multiplied by $q^2/\log(q/\pi)$ as a function of $|q|$ [along the $(1,0)$ direction] for different U/t and the same sizes as Fig. 7.
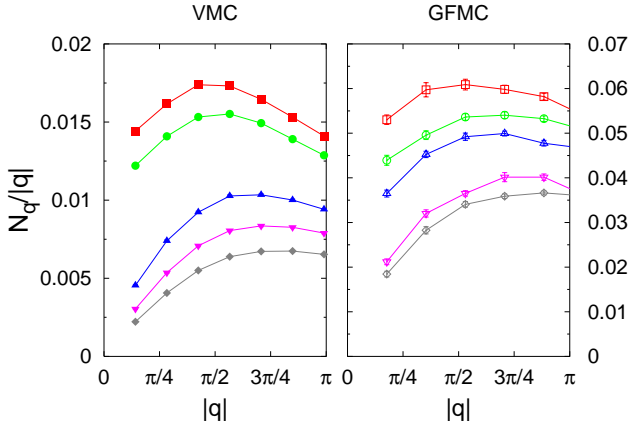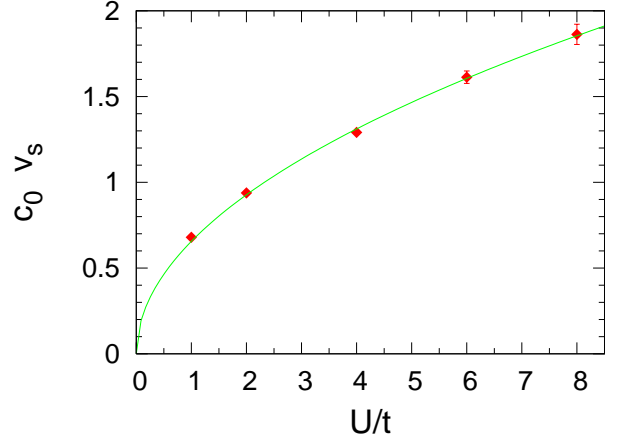

FIG. 10: GFMC results for the sound velocity v_c obtained through a finite size scaling of the ground-state energy, see Eq. (19). The line is a guide to the eyes.
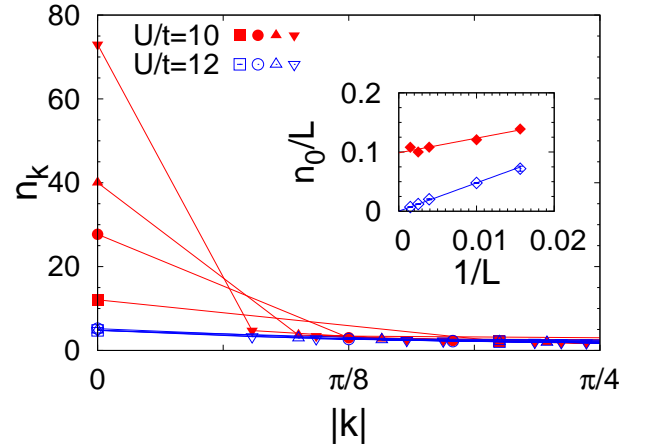

FIG. 9: Left panel: Density structure factor N_q divided by $|q|$ calculated by the variational Monte Carlo for different U/t and $L = 20 \times 20$. From top to bottom $U/t = 10$, 10.2, 10.4, 11, and 12. Right panel: The same for the GFMC on the $L = 16 \times 16$ cluster. From top to bottom $U/t = 8$, 8.2, 8.4, 8.6, and 8.8.

FIG. 11: Variational results for the momentum distribution $\mathbf{n}_k$ in 2D for 10×10 (squares), 16×16 (circles), 20×20 (upward triangles), and 26×26 (downward triangles) clusters with $U/t = 10$ and 12. Inset: Size scaling of the condensate fraction $\mathbf{n}_0/L$ for $U/t = 10$ (upper curve) and $U/t = 12$ (lower curve).

than the one obtained by the simple Gutzwiller wave function, for which $U_c/t \sim 11.65$.[14] The critical value of the on-site interaction is rather different within GFMC, yielding $U_c/t \sim 8.5 \pm 0.1$, in close agreement with the value found in the literature.[9] Let us focus more deeply on the behavior of the structure factor N_q. Approaching the transition from the weak-coupling region, γ_1 goes smoothly to zero, in contrast with the results of the 1D model, where we observed an abrupt jump. Also contrasting the 1D case, γ_2 is found to be finite and continuous across the transition. These results, based upon the variational wave function, are confirmed by the GFMC calculations, see Fig. 9. The vanishing linear coefficient of N_q can be ascribed either to v_s or to χ. In order to clarify which one of these quantities goes to zero at the transition, we extract the sound velocity v_s from the

finite-size scaling of the exact ground-state energy by

$$\epsilon_0(L) = \epsilon_0(\infty) - \frac{c_0 v_s}{l^3}, \qquad (19)$$

where $\epsilon_0(L)$ is the ground-state energy per site for a cluster with $L = l^2$ sites, $\epsilon_0(\infty)$ is the extrapolated value in the thermodynamic limit, and c_0 is a given model-dependent constant. Our results, shown in Fig. 10, clearly indicate that v_s stays finite across the superfluid-insulator transition, thus implying a vanishing compressibility when approaching the insulator.

The fingerprint of this transition is also given by the momentum distribution, see Fig. 11. For this quantity, a striking difference is observed below and above U_c. In the former case, a cusp-like behavior with a finite condensate
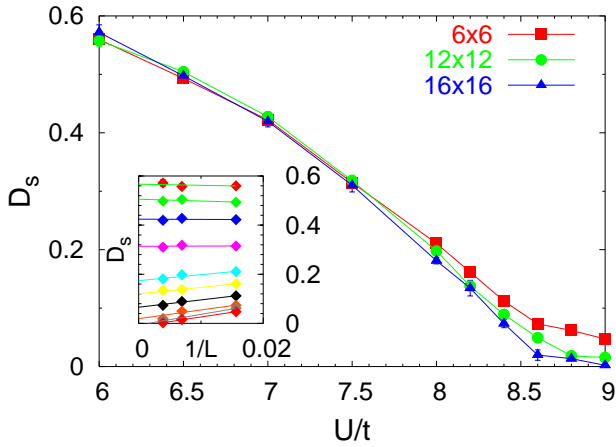
FIG. 12: Superfluid stiffness D_s as a function of U/t for different sizes. Inset: Size scaling of D_s for different U/t (the same values of the main panel are reported, with U/t increasing from top to bottom).
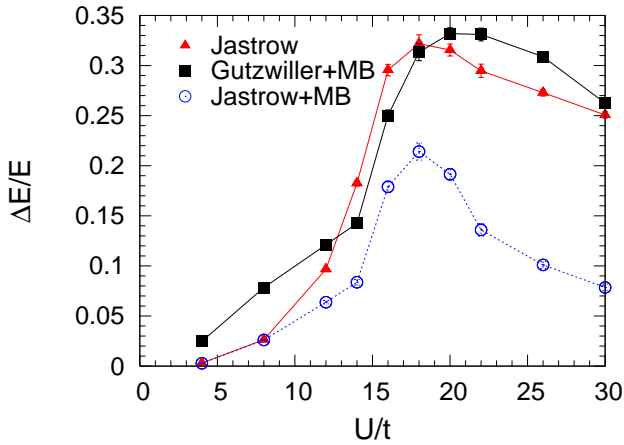

FIG. 13: Accuracy of different variational wave functions as a function of U/t for the $10 \times 10 \times 10$ cluster and 1000 bosons. The symbols are the same as in Fig. 1.

FIG. 14: Jastrow parameters v_q multiplied by $|q|^3$ as a function of $|q|$ for $8 \times 8 \times 8$ (circles), $10 \times 10 \times 10$ (squares), and $12 \times 12 \times 12$ (triangles) clusters [along the (1,0,0) direction].

FIG. 15: Upper panel: Variational results for the density structure factor N_q for 3D and $U/t = 20$. Lower panels: N_q for non-optimized wave functions with $v_q \sim \beta_{3D}/|q|^3$ for two values of β_{3D}.

fraction is found, whereas in the latter case a smooth behavior is detected, with a vanishing n_0/L. Notice that a vanishing condensate fraction in the thermodynamic limit immediately follows from $N_q \sim q^2$ by using the f-sum rule derived in Ref. 36.

Finally, we report in Fig. 12 the stiffness D_s, calculated by using GFMC. In 2D, we obtain a different behavior with respect to the 1D case, where a finite jump is rather clear at the superfluid-insulator transition. Indeed, the evaluation of the stiffness for different sizes confirms the absence of the jump in 2D, as expected for a second order phase transition.[9]
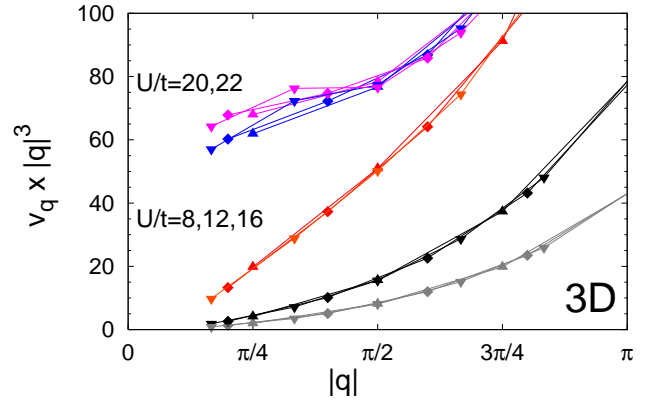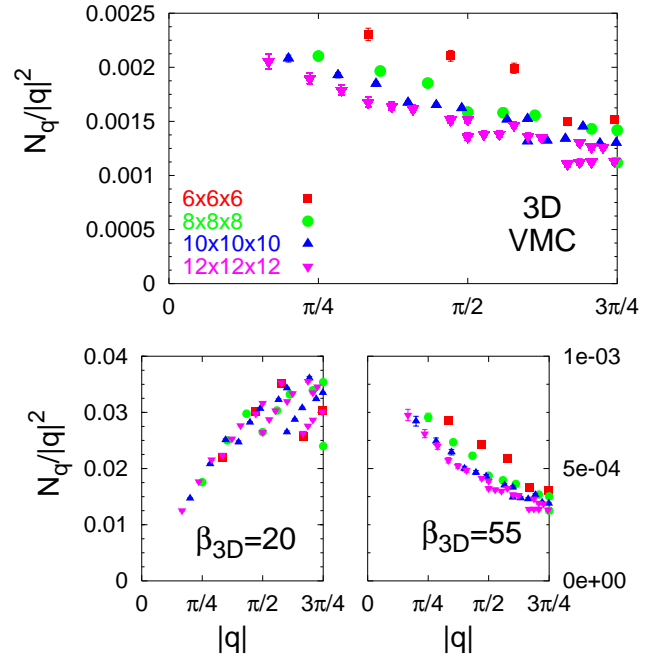
V. THE 3D HUBBARD MODEL

Let us move now to the 3D case. Here, we mostly restrict our analysis to the variational method that allows us to assess rather large sizes. We start by considering the accuracy of the different variational states as a function of the interaction U/t, see Fig. 13. It turns out that in the large-U region the most accurate state contains both the long-range Jastrow term and the many-body term, as it occurs in 2D. Moreover, in analogy to 1D and 2D,

the presence of a phase transition upon increasing U/t is clearly signaled by the sudden change in the small-q behavior of the Jastrow factor, see Fig. 14. Here, its behavior changes drastically from $v_q \sim \alpha/|q|$ to a more diverging $v_q \sim 1/|q|^3$ in the insulating regime. In particular, the sudden change of behavior allows us to locate the transition around $U_c/t \simeq 18$, which is close to the critical value of recent Monte Carlo simulations.[10]

Focusing on the large-U region of the phase diagram, let us discuss the implications of the singular $v_q \sim 1/|q|^3$ Jastrow potential. First of all, following the same arguments of Ref. 32, we can assert that the strong singular character of the Jastrow potential is able to empty the condensate, whereas a less singular $v_q \sim 1/q^2$ would not lead to $n_0 \to 0$ in the thermodynamic limit. Remarkably, even though $v_q \sim 1/|q|^3$, the structure factor in the insulator has the correct $N_q \sim q^2$ behavior, see Fig. 15. In turn, this implies that Eq. (15) does not hold. In order to prove more firmly that $v_q \sim \beta_{3D}/|q|^3$ can indeed lead to $N_q \sim q^2$, we have calculated the density structure factor with a *non-optimized* wave function of the form (5) with $v_q \sim \beta_{3D}/|q|^3$ and for different values of β_{3D}. As shown in Fig. 15, for small β_{3D} we obtain $N_q \sim |q|^3$, implying that Eq. (15) is qualitatively correct in this case. However, above a critical β_{3D}^*, the small-q behavior of the density structure factor turns into $N_q \sim q^2$, signaling a remarkable breakdown of Eq. (15). From Fig. 14 it turns out that the optimal value of β_{3D} that we get variationally at the superfluid-insulator transition is larger than β_{3D}^*, confirming that $N_q \sim q^2$ in the insulating phase. Most importantly, the change of behavior as a function of β_{3D} is consistent with the binding-unbinding phase-transition recently uncovered in a classical 3D gas with a $1/|q|^3$ potential.[33] Once again, as in 1D and 2D, the Mott insulating wave function in 3D is found to be closely related to the low-temperature confined phase of a classical model, where opposite charges tightly bound.

VI. 2D SYSTEMS WITH LONG-RANGE INTERACTION

In the previous paragraphs, we have shown that, in the Hubbard model (1), the superfluid regime can be described by a long-range Jastrow wave function with $v_q \sim \alpha/|q|$. By increasing the on-site interaction U, our variational approach describes a continuous transition to an insulating phase that corresponds to the confined phase of a classical model of interacting particles with opposite charge. In particular, we have found evidences that the 2D Mott insulating wave function corresponds to a classical model with $-\log(q)/q^2$ potential rather than to a 2D CGM with potential β/q^2 in the confined phase ($\beta > \beta^* \geq 4\pi$). This result, as we discussed, has a physical importance since the confined 2D CGM has power-law correlations, not possible in a Mott insulating phase. Nevertheless, it would be interesting to search for bosonic Hamiltonians whose ground state can
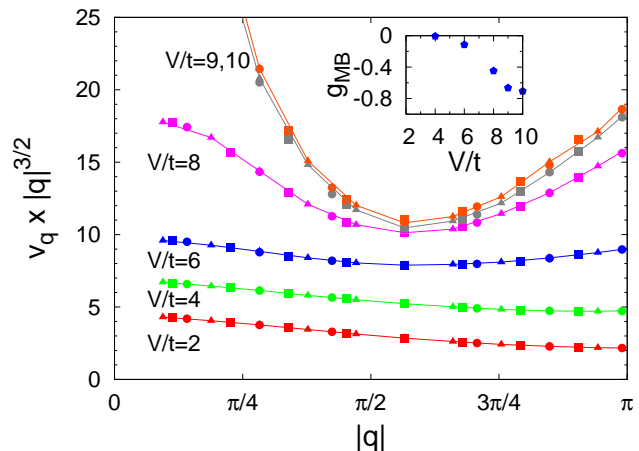
FIG. 16: Jastrow parameters v_q multiplied by $|q|^{3/2}$ as a function of $|q|$ for the potential of Eq. (3) with different V/t and 20×20 (circles), 26×26 (squares), and 30×30 (triangles) clusters. Inset: The many-body variational parameter g_{MB} as a function of V/t.
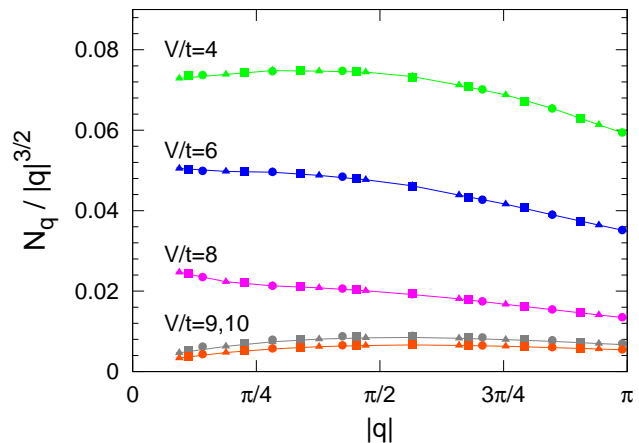
FIG. 17: Variational results for the density structure factor $N(q)$ divided by $|q|^{3/2}$ for the potential of Eq. (3) with different V/t and 20×20 (circles), 26×26 (squares), and 30×30 (triangles) clusters.

be described by the variational wave function (8) with a Jastrow potential $v_q \sim \beta/q^2$.

For that purpose, we consider the more general Hubbard model of Eq. (2) with a long-range interaction $\Omega(r)$. Let us start by considering the realistic case of a Coulomb potential, namely $\Omega(r) \sim 1/r$ that in 2D leads to Eq. (3). Then, we can vary its strength V to drive the system across a superfluid-insulator transition. The small-q behavior of the optimized Jastrow parameters is shown in Fig. 16. For $V/t \lesssim 8$, we obtain that $v_q \sim 1/|q|^{3/2}$. On the contrary, for larger values of the interactions, v_q becomes more singular and in particular is best fitted by $-\log(q)/q^2$, just like what we found for short-range interaction. The structure factor in the weak-coupling phase behaves as $N_q \sim |q|^{3/2}$, see Fig. 17, compatible with a
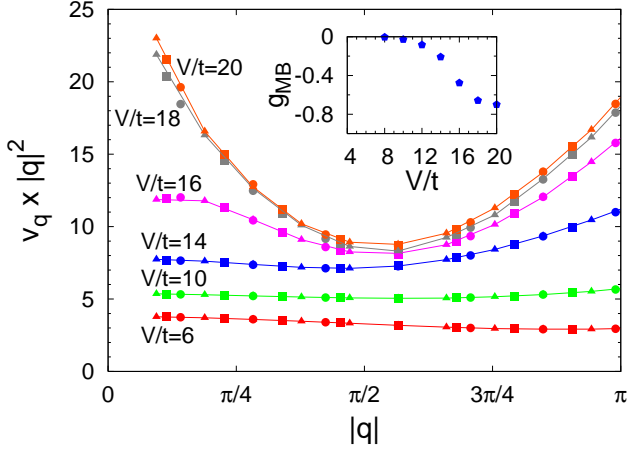
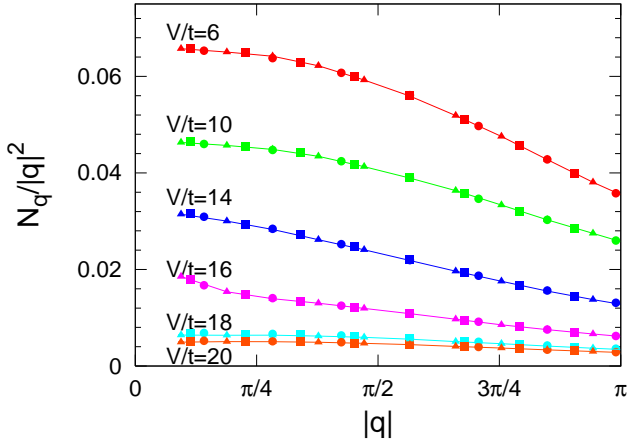FIG. 18: The same as in Fig. 16, for the potential of Eq. (4).

FIG. 19: The same as in Fig. 17, for the potential of Eq. (4).

superfuid phase with 2D plasmons. We mention that a similar behavior has been found in continuum models at high densities both analytically[37] and numerically.[38] In the strong-coupling regime, the insulating behavior $N_q \sim q^2$ is recovered. These results are confirmed by GFMC (not shown), though the critical V/t is slightly decreased, i.e., $V_c/t \sim 7$. In this case, as before with short-range interaction, the optimized Jastrow never behaves as the potential of a CGM.

Therefore, let us turn to the more singular interaction given by Eq. (4), leading to $\Omega(r) \sim -\log(r)$. In this case the potential in q-space is given by $\Omega(q) \sim 1/q^2$ and we expect, similarly to what happens in the continuum for high density,[21] that in the weak-coupling regime also $v_q \sim \beta/q^2$. Indeed, as shown in Fig. 18, this is the case for $V/t \lesssim 16$. Above this value, v_q becomes once again of the form $-\log(q)/q^2$, just like in all previous examples. We note that the values of β extracted in the weak coupling phase seem to be all smaller than β^* of the 2D Berezinskii-Kosterlitz-Thouless phase transition, although we can not exclude by the numerical data that

$\beta \to \beta^*$ at the transition. This indicates that the CGM that corresponds to the variational wave function is in the plasma phase, with exponential decaying density-density correlation functions. Indeed, the structure factor behaves like $N_q \sim q^2$ for all the coupling strengths V/t, see Fig. 19. We believe that the weak-coupling phase has to be identified with the algebraic long-range ordered phase found at high density in the continuum model by Magro and Ceperley.[21] This phase is characterized by absence of condensate but by a power-law decay of the single-particle density matrix. On the contrary, the strong-coupling phase with Jastrow potential $v_q \sim -\log(q)/q^2$ must correspond to a genuine Mott insulator with all correlation functions decaying exponentially.

VII. CONCLUSIONS

We have shown that the long-range Jastrow wave function gives a consistent picture of the superfluid-insulator transition of the bosonic Hubbard model in all spatial dimensions and also in the presence of long-range interaction.

In one dimension the variational results are compatible with a Berezinskii-Kosterlitz-Thouless phase transition between the quasi-long-range ordered gapless phase and the Mott insulator. From the point of view of the variational wave function, the gapless phase is characterized by a Jastrow potential $v_q \sim \alpha/|q|$, while the insulating one by $v_q \sim 1/q^2$.

In two dimensions we have evidences of a second-order phase transition between a superfluid phase and a Mott insulator. Here, the superfluid wave function still has $v_q \sim \alpha/|q|$, compatible with the existence of sound modes, while the insulating wave function is characterized by a more singular $v_q \sim -\log(q)/q^2$. This singular behavior in the Mott phase does not change even if long-range interaction is considered. For instance, for a Coulomb interaction $\Omega(r) \sim 1/r$, the Jastrow potential in the superfluid phase changes into $v_q \sim 1/|q|^{3/2}$, compatible with the existence of 2D plasmons, yet the insulating wave function has still $v_q \sim -\log(q)/q^2$. For an interaction $\Omega(r) \sim \log(r)$, we observe a transition between an algebraic long-range ordered phase,[21] characterized by $v_q \sim 1/q^2$, and a Mott insulating phase, once again with $v_q \sim -\log(q)/q^2$.

In three dimensions, the Mott transition as revealed by the behavior of the Jastrow potential becomes much more evident. As usual, the superfluid phase has $v_q \sim \alpha/|q|$. In this case, however, the Mott insulating wave function has a much more singular $v_q \sim 1/|q|^3$, still with a structure factor that correctly behaves as $N_q \sim q^2$.

This work was mainly focused on bosons, but a similar variational wave function can be applied also to fermionic models, with the same key ingredient, i.e., a long-range Jastrow factor that drives the metal-insulator transition, in spite of the uncorrelated wave function being metallic.[15,17] According to this picture, the Mott insulating

state should be produced by a sufficiently long-range Jastrow potential able to bind opposite-charge fluctuations. Based on the bosonic results, we may argue that a Jastrow potential $v_q \sim 1/|q|^D$ may work even for fermions in any dimensions $D > 2$, $D = 2$ playing somehow the role of the lowest critical dimension, $v_q \sim -\log(q)/q^2$. As the interaction strength is decreased, an unbinding transition must takes place in the variational wave function, turning the Mott insulator into a correlated metal and providing a simple physical picture of the long-standing but still actual and very attractive phenomena which is the Mott transition.

APPENDIX A: DETAILS FOR THE CALCULATION OF THE STIFFNESS

In this Appendix, we give some details for the zero-temperature GFMC calculation of the stiffness D_s. In this respect, we consider the standard Peierls substitution and introduce an electromagnetic field in the Hamiltonian by replacing the hopping term between two sites R_i and R_j by a suitable complex hopping:[39]

$$t \to t \exp\left\{ i \int_{R_i}^{R_j} dR\, A(R) \right\}, \qquad (A1)$$

where we can consider $A(R) = (A_x, 0)$. Then, the first derivative of the energy $E[A]$ with respect to this field gives the charge current, containing both the paramagnetic and diamagnetic contributions. This current must vanish when $A_x \to 0$, since the Hamiltonian is real. For a bosonic system, the second derivative of the energy $E[A]$ represents the charge stiffness.[40]

Within GFMC it is possible to compute the ground-state energy $E[A]$ for arbitrary time-independent static field A_x. Let us denote by $\mathcal{H}_A$ and $\mathcal{H}$ the Hamiltonian in presence and absence of the field, respectively and consider:

$$Z_\tau[A] = \frac{1}{\tau} \frac{\langle \Phi | e^{-\tau \mathcal{H}_A} | \Psi_0 \rangle}{\langle \Phi | e^{-\tau \mathcal{H}} | \Psi_0 \rangle}, \qquad (A2)$$

where $|\Psi_0\rangle$ is the ground state of $\mathcal{H}$, with E_0 energy, and $|\Phi\rangle$ is the guiding wave function of the GFMC method. In the large-τ limit, we have that

$$Z_\tau[A] \sim \frac{1}{\tau} \frac{\langle \Phi | \Psi_0^A \rangle \langle \Psi_0^A | \Psi_0 \rangle}{\langle \Phi | \Psi_0 \rangle} \, e^{-\tau(E_0^A - E_0)}, \qquad (A3)$$

where $|\Psi_0^A\rangle$ and E_0^A are the ground state eigenfunction and eigenvalue of $\mathcal{H}_A$, respectively. By taking the second derivative of $Z_\tau[A]$ with respect to A and then considering $A = 0$, we obtain the charge stiffness (up to $1/\tau$ corrections).

This quantity can be obtained by sampling statistically the unperturbed Green's function $G_{x',x} = -\Phi_{x'}\mathcal{H}_{x',x}/\Phi_x = p_{x',x}b_x$, where $p_{x',x}$ is a stochastic matrix that defines the Markov chain and b_x is a normalization factor. In this way, the walker $|x\rangle$ is distributed according to the variational distribution $|\langle x|\Phi\rangle|^2$ and, in order to obtain the true ground state, the weight G^τ must be considered. Then

$$Z_\tau[A] = \frac{1}{\tau} \frac{\sum_n G_n^\tau[A]}{\sum_n G_n^\tau} \qquad (A4)$$

where the index n indicates the Markov chain iteration, that is defined by the transition probability $p_{x',x}$, and

$$G_n^\tau = \exp\left\{ \int_0^\tau d\tau'\, e_L[x(\tau')] \right\} \qquad (A5)$$

$$G_n^\tau[A] = G_n^\tau \exp\left\{ i \int_{R_{x(0)}}^{R_{x(\tau)}} dR\, A(R) \right\} \qquad (A6)$$

are the correcting factors of the GFMC method; $e_L(x)$ indicates the local energy and R_x indicates the site where the particle moves within the GFMC algorithm. By considering the second derivative of $Z_\tau[A]$ with respect to A_x, we obtain Eq. (18). As usual, many walkers can be considered with the branching technique in order to reduce the variance of the correcting factors G_n^τ.

[1] D. Jaksch, C. Bruder, J.I. Cirac, C.W. Gardiner, and P. Zoller, Phys. Rev. Lett. **81**, 3108 (1998).

[2] M. Greiner, O. Mandel, T. Esslinger, T.E. Hansch, and I. Bloch, Nature (London) **415**, 39 (2002).

[3] W. Zwerger, J. Opt. B: Quantum Semiclassical **5**, S9 (2003).

[4] M.P.A. Fisher, P.B. Weichman, G. Grinstein, and D. Fisher, Phys. Rev. B **40**, 546 (1989).

[5] G.G. Batrouni, R.T. Scalettar, and G.T. Zimanyi, Phys. Rev. Lett. **65**, 1765 (1990).

[6] G.G. Batrouni and R.T. Scalettar, Phys. Rev. B **46**, 9051 (1992).

[7] T.D. Kuhner and H. Monien, Phys. Rev. B **58**, R14741 (1998).

[8] T.D. Kuhner, S.R. White, and H. Monien, Phys. Rev. B **61**, 12474 (2000).

[9] W. Krauth and N. Trivedi, Europhys. Lett. **14**, 627 (1991).

[10] B. Capogrosso-Sansone, N.V. Prokof'ev, and B.V. Svistunov, Phys. Rev. B **75**, 134302 (2007).

[11] J.K. Freericks and H. Monien, Phys. Rev. B **53**, 2691 (1996).

[12] N. Elstner and H. Monien, Phys. Rev. B **59**, 12184 (1999).

[13] D.S. Rokhsar and B.G. Kotliar, Phys. Rev. B **44**, 10328 (1991).

[14] W. Krauth, M. Caffarel, and J. Bouchaud, Phys. Rev. B **45**, 3137 (1992).

[15] M. Capello F. Becca, M. Fabrizio, S. Sorella, and E. Tosatti, Phys. Rev. Lett. **94**, 026406 (2005).

[16] M. Capello, F. Becca, S. Yunoki, M. Fabrizio, and S. Sorella, Phys. Rev. B **72**, 085121 (2005).

[17] M. Capello, F. Becca, S. Yunoki, and S. Sorella, Phys. Rev. B **73**, 245116 (2006).

[18] M. Capello, F. Becca, M. Fabrizio, and S. Sorella, Phys. Rev. Lett. **99**, 056402 (2007).

[19] N. Trivedi and D.M. Ceperley, Phys. Rev. B **41**, 4552 (1990).

[20] M. Calandra and S. Sorella, Phys. Rev. B **57**, 11446 (1998).

[21] W.R. Magro and D.M. Ceperley, Phys. Rev. Lett. **73**, 826 (1994).

[22] W.R. Magro and D.M. Ceperley, Phys. Rev. B **48**, 411 (1993).

[23] H. Nordborg and G. Blatter, Phys. Rev. Lett. **79**, 1925 (1997).

[24] S. Sorella, Phys. Rev. B **64**, 024512 (2001).

[25] H. Yokoyama and H. Shiba, J. Phys. Soc. Jpn. **59**, 3669 (1990)

[26] H. Yokoyama and M. Ogata, arXiv:0708.2765.

[27] R. Roth and K. Burnett, J. Phys. B **37**, 3893 (2004).

[28] R.P. Feynman and M. Cohen, Phys. Rev. **102**, 1189 (1956).

[29] L. Reatto and G.V. Chester, Phys. Rev. **155**, 88 (1967).

[30] P. Minnhagen, Rev. Mod. Phys. **59**, 1001 (1987).

[31] A. Lenard, J. of Math. Phys. **2**, 682 (1961).

[32] L. Reatto, Phys. Rev. **183**, 334 (1969)

[33] S. Kragset, A. Sudbo, and F.S. Nogueira, Phys. Rev. Lett. **92**, 186403 (2004).

[34] N. Laflorencie, S. Capponi, and E.S. Sorensen, Eur. Phys. J. B **24**, 77 (2001).

[35] E.L. Pollock and D.M. Ceperley, Phys. Rev. B **36**, 8343 (1987).

[36] L. Pitaevskii and S. Stringari, J. Low Temp. Phys. **85**, 377 (1991); Phys. Rev. B **47**, 10915 (1993).

[37] V. Apaja, J. Halinen, V. Halonen, E. Krotscheck, and M. Saarela, Phys. Rev. B **55**, 12925 (1997).

[38] S. De Palo, S. Conti, and S. Moroni, Phys. Rev. B **69**, 035109 (2004).

[39] R.E. Peierls, Z. Phys. **80**, 763 (1933).

[40] W. Kohn, Phys. Rev. **133**, A171 (1964).